Theoretical and Experimental Characterization of Cr−L Multiple Bonds (L = O, N, and C)

Chih-Chieh Wang,[†,‡,§] Ting-Hua Tang,[†] and Yu Wang*[,†]

Department of Chemistry, National Taiwan University, Taipei, Taiwan, Republic of China, and Department of Chemistry, Soochow University, Taipei, Taiwan, Republic of China

Received: March 27, 2000; In Final Form: August 4, 2000

A combined experimental and theoretical study on the bond characterization of Cr−L (L = O, N, C) multiple bonds is applied to a series of Cr-complexes: $[(CO)_4(Cl)Cr^{(I)}(CPh)]$ **1**; $[Cr^{(V)}(N)(bpb)]$ **2**, and $[Cr^{(V)}(N\text{-}t\text{-}Bu)(bpb)(Cl)]$ **3**, where [bpb^{2-} = (1,2-bis(pyridine-2-carboxamido)benzene)]; and $[(TPPOMe)Cr^{(IV)}O]$ **4**, where [TPPOMe = (5,10,15,20-*p*-methoxyphenyl)porphyrin)]. Compounds **1** and **2** were investigated by accurate single-crystal X-ray diffraction. Detailed descriptions of $Cr-C_{carbyne}$, $Cr-N_{nitrido}$, $Cr-N_{imido}$, and $Cr-O_{oxo}$ bonds will be given based on the natural bonding orbital (NBO) analyses and Fermi hole function. The bonding feature of all these multiple bonds is essentially a triple bond character consisting of one σ and two π bonds. The σ character of the Cr−L multiple bonds is a highly polarized one with the electron density strongly polarized toward L (O, N, C) ligands. The π character of the Cr−L multiple bonds depends on the nature of L ligand, i.e., with electron density polarized toward the Cr and O center for $Cr-C_{carbyne}$ and $Cr-O_{oxo}$ bond, respectively, whereas electron density is roughly equally distributed at both Cr and N for the $Cr-N_{nitrido}$ and $Cr-N_{imido}$ bonds. Bond characterizations are also shown in terms of Laplacian of electron density where the inner valence shell charge concentration (i-VSCC) is embedded. The isovalue surface of zero Laplacian of electron density reveals the shape of such i-VSCC at each chromium atom. Shapes around the Cr atom are a pressed disklike for **1** and **3** and inverted square pyramid for **2** and **4**. The topological properties associated with the bond critical point (BCP) of Cr−L multiple bonds in these compounds indicate a strong covalent bond character. The order of the binding interaction is $Cr-N_{nitrido} > Cr-O_{oxo} > Cr-N_{imido} > Cr-C_{carbyne}$. The combined study of experiment and theory on **1** and **2** demonstrates good agreement between experiment and theory.

Introduction

Chemical bonding is a very important concept in understanding molecular behavior. Bond characterization is therefore becoming ever needed for predicting the physical and chemical properties of molecules. Combined experimental and theoretical studies[1−6] has been used for such a purpose in terms of deformation density distribution and natural bond orbital analysis. Such studies do provide qualitative description of bonding type. However, the drawback in this method is the bias[7−10] on the definition of the promolecule. The topological analysis of "Atoms in Molecules" theory[11] brings in new insight on chemical bonding characterization. The bias on how to treat properly the promolecule model is no longer a problem since the topological properties analysis is based entirely on the total electron density of the molecule. Deformation density studies of Cr-complexes[12−14] have revealed important aspects on the bonding features of various types of Cr−L multiple bonds. To give a quantitative description of the Cr−L multiple bond, four Cr-complexes, $[(CO)_4(Cl)Cr^{(I)}(CPh)]$ **1**,[12] $[Cr^{(V)}(N)(bpb)]$ **2**,[13] $[Cr^{(V)}(N\text{-}t\text{-}Bu)(bpb)(Cl)]$ **3**,[14] and $[(TPPOMe)Cr^{(IV)}O]$ **4**,[14] with the $Cr-C_{carbyne}$, $Cr-N_{nitrido}$, $Cr-N_{imido}$, and $Cr-O_{oxo}$ bond are chosen to be investigated by the topological analysis of the electron density distribution,[11] natural bond orbital (NBO)[15] analysis, and Fermi hole distribution.[16−18] The topological properties associated with the BCP for various types of Cr−ligand bond are compared and discussed in detail between experiment and theory. The inner valence shell charge concentrations (i-VSCCs)[19,20] of Cr atoms associated with their geometrical conformation are also investigated.

Computational Details

The geometries of compound **1**, **2**, **3,** and **4** used for the theoretical calculations are taken from the diffraction data.[12−14] Simplified model compound **3** [(Cl)(bpb)Cr(NCH_3)] and **4** [(porphyrin)CrO] are used for the theoretical calculations. All computations are performed using the B3LYP hybrid HF/DFT method[21] with the G98 program package.[22] The basis set contraction used for Cr atom is (62111111)/5112/411).[23,24] The (14s, 9p) primitive Gaussian functions are taken from Wachters[23] and (6d) basis set are taken from Goddard.[24] The 6-31G* basis set[22] was used for Cl, N, O, C, and H. The importance of electron correlation of transition metal system has been reported.[25−27] The DFT includes electron correlation effect empirically and is claimed[25,26] to have comparable accuracy as post-Hartree−Fock methods. However, it was reported[28] that the topological properties of the electron density are not qualitatively affected by the inclusion of electron correlation. The quantitative changes at the critical points in both $\rho(r)$ and

* Author to whom correspondence should be addressed. Telephone: 886-2-23630231, ext 2325. Fax: 886-2-23636359. E-mail: yuwang@xtal.ch.ntu.edu.tw.
† National Taiwan University.
‡ Soochow University.
§ E-mail: ccwang@mail.scu.edu.tw.

10.1021/jp001130x CCC: $19.00
Published on Web 10/03/2000

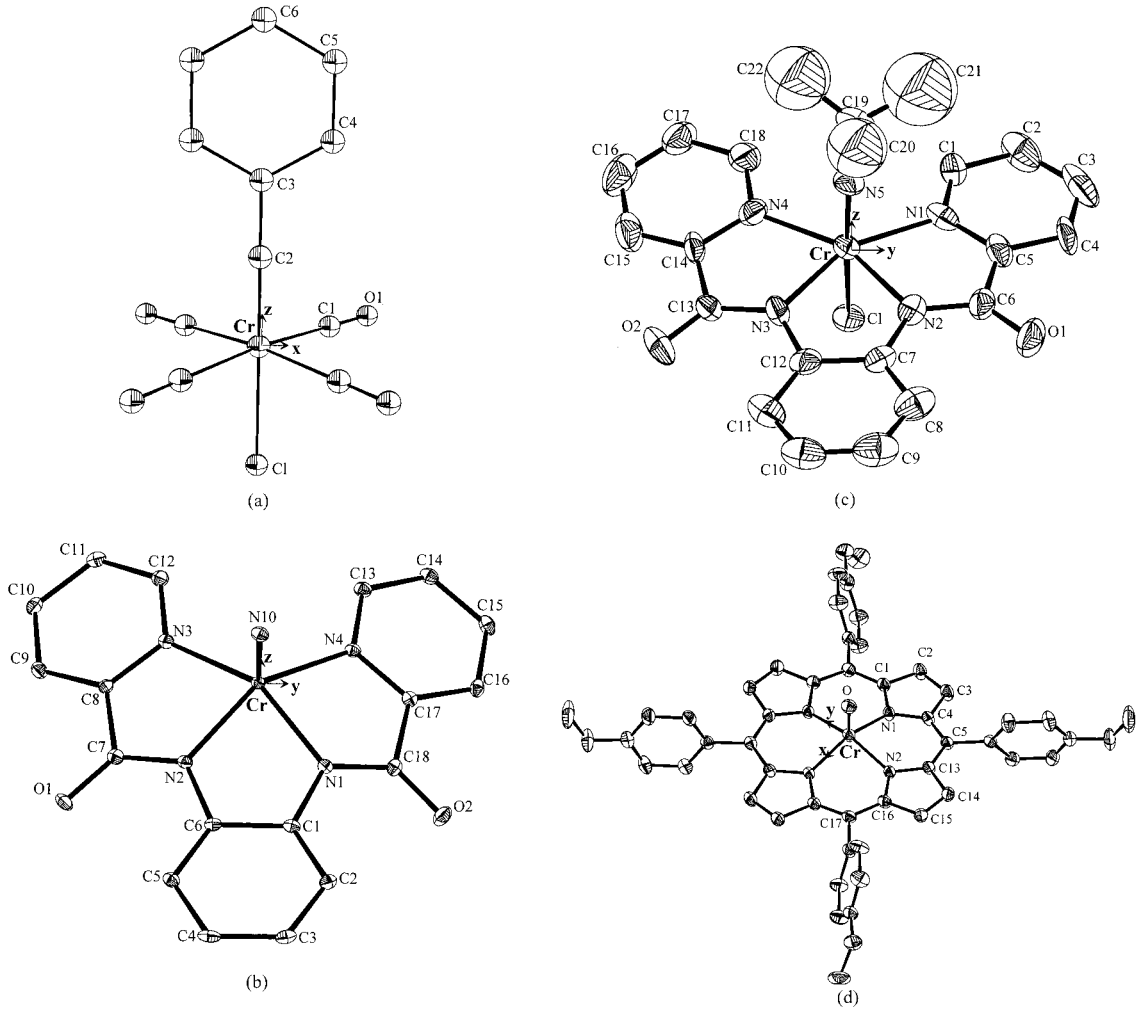

Figure 1. Molecular structures of compound (a) **1**, (b) **2**, (c) **3,** and (d) **4**.

$\nabla^2\rho(r)$ induced by correlation are found to be small in magnitude.

The topological property analysis on electron density is based on Bader's "Atoms in Molecules (AIM)" theory.[11] Total electron density obtained from the experiment is calculated according to the multipole model[29] and the multipole coefficients (P_{lm}'s) and the single kappa values of **1** and **2** are taken from the literature.[12,13] The multipole terms of Cr atom are up to hexadecapole (total number of 25) for both **1** and **2**. Total electron density from the theory is calculated on the basis of the DFT calculation. Maps of Laplacian, charge distribution, and the other topological properties are obtained using the PROP[30] and AIMPAC[31] programs for experiment and theory, respectively.

Result and Discussion

Structures. The crystal structures and deformation density distribution of **1**, **2**, **3,** and **4** have been reported.[12−14] The coordination spheres of Cr center are either in an octahedral (**1** and **3**) or in a square pyramidal (**2** and **4**) geometry. The molecular structure and the local coordinates of Cr atom for compound **1**, **2**, **3,** and **4** are shown in Figure 1. Compound **1** is a typical low-valent carbyne complex with the $Cr-C_{carbyne}$ distance of 1.724(1) Å.[12] Compounds **2** and **3** are both high-valent Cr complexes with Cr−N distance of 1.555(2) and 1.63(1) Å for nitrido **2** and imido **3** complex.[13,14] The Cr atom is located at 0.519 and 0.173 Å above the equatorial plane of the tetradentate of bpb^{2-} ligand for **2** and **3**, respectively. Compound **4** is a five-coordinated complex with $Cr-O_{oxo}$ bond of 1.588(4) Å. The Cr atom is located 0.434 Å above the plane of porphyrin ligand.[14] Selected bond distances of various Cr−L bond are listed in Table 1. There are various types of Cr−N bonds in these four complexes, where the bond length is in the order of $Cr-N_{nitrido} < Cr-N_{imido} < Cr-N_{amido} < Cr-N_{pyridine} \cong Cr-N_{pyrole}$.

NBO Analysis. The natural bond orbital analyses (NBO) of four types of Cr−L multiple bonds ($Cr-C_{carbyne}$, $Cr-N_{nitrido}$, $Cr-N_{imido}$, and $Cr-O_{oxo}$) are listed in Table 2. Each one is described in terms of bond type (σ, π), natural hybrid orbital (NHO) at each bonded atomic center as well as the electron occupancy of the bond. It is clear that all of the Cr−L multiple bonds are a triple bond character with one σ and two π bonds. The calculated bond orders are 2.44, 2.72, 2.40, and 2.65 for $Cr-C_{carbyne}$, $Cr-N_{nitrido}$, $Cr-N_{imido}$, and $Cr-O_{oxo}$ bonds, respectively. The σ bond of Cr−L multiple bond is formed by a sd_{z^2} hybrid orbital of Cr and a sp_z hybrid of L with major contribution (60−80%) from L. The π bonds of Cr−L are formed by d_π (d_{xz}, d_{yz}) orbitals of Cr and p_π (p_x, p_y) orbitals of L. In the cases of $Cr-N_{nitrido}$ and $Cr-N_{imido}$ bonds in **2** and **3**, both π bonds are formed with equal contribution from p_π orbital of $N_{nitrido/imido}$ and d_π orbitals of Cr, though p_π of N_{imido} does contribute slightly more than d_π of Cr in **3**. In the case of $Cr-O_{oxo}$ bond in **4**, the p_π orbital of O contributes much more than the d_π orbitals of Cr on $Cr-O_{oxo}$ π bond. But, in the case of

TABLE 1: Selected Cr−L Bond Length and Topological Properties Associated with BCP of 1, 2, 3, and 4 (for 1 and 2, first line from experiment, second line from theory)

bonds/B.L. (Å)	$d1$[a] Å	ρ(r) e Å^{-3}	$\nabla 2\rho$(r)[b] e Å^{-5}	H_b[c] Hartree/Å^3
		1		
Cr−Cl	1.242	0.183	3.047	
2.409(1)	1.084	0.377	4.442	−0.040
Cr−C1$_{carbonyl}$	0.972	0.824	11.520	
1.957(1)	0.959	0.675	11.043	−0.137
Cr−C2$_{carbyne}$	0.895	0.859	11.520	
1.724(1)	0.896	1.228	13.881	−0.618
		2		
Cr−N1$_{amido}$	0.990	0.721	11.686	
1.967(2)	0.968	0.699	9.801	−0.107
Cr−N3$_{pyridyl}$	1.033	0.537	8.292	
2.080(2)	1.003	0.514	8.853	−0.015
Cr−N10$_{nitrido}$	0.846	1.873	26.940	
1.555(2)	0.842	2.057	13.54	−1.728
		3		
Cr−Cl	1.096	0.373	3.716	−0.047
2.432(6)				
Cr−N1$_{pyridyl}$	0.999	0.553	8.734	−0.032
2.063(16)				
Cr−N2$_{amido}$	0.963	0.743	9.641	−0.133
1.961(14)				
Cr−N5$_{imido}$	0.847	1.477	23.918	−0.823
1.634(14)				
		4		
Cr−N1$_{pyrrole}$	0.977	0.562	10.374	−0.024
2.025(3)				
Cr−O$_{oxo}$	0.815	1.827	23.539	−1.239
1.588(4)				

[a] $d1$: distances from BCP to the first atom of the bond. [b] Laplacian at critical point (BCP), $\nabla^2\rho(\mathbf{r}_c) = (\lambda_1 + \lambda_2 + \lambda_3)$. [c] H_b: total energy density at BCP.

Cr−C$_{carbyne}$ in **1**, it is just the opposite that the d_π orbital of Cr contributed much more than the p_π orbital of C atom. This trend is nicely correlated with their relative atomic electronegativity. On the basis of such orbital analysis, one denotes that the orbital energies of p_π orbitals of the L ligand and of d_π orbitals of Cr are in the order of

$$p_\pi\,(O_{oxo}) < p_\pi\,(N_{imido}) < p_\pi\,(N_{nitrido}) \cong d_{xz,yz}\,(Cr) < p_\pi\,(C_{carbyne})$$

The π orbital interaction between the Cr (d_{xz}, d_{yz}) orbitals and L (p_x, p_y) orbitals can be described as follows:

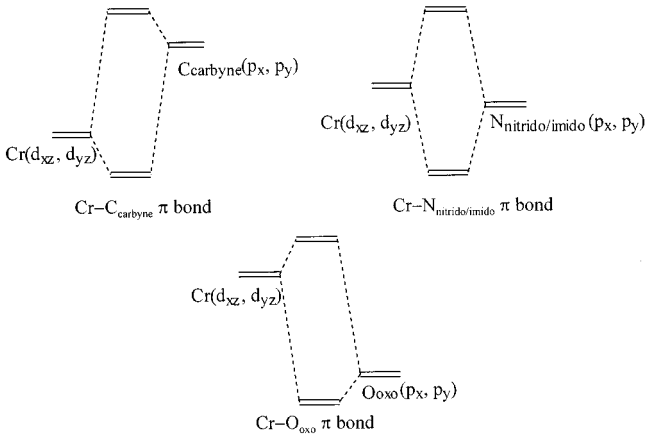

According to NBO population analysis, the Cr−C$_{carbyne}$ π bond density is polarized toward the Cr atom, while the σ density is mainly from C$_{carbyne}$. This result is consistent with the NBO analysis on the W−C$_{carbyne}$ bond.[32a] In the case of Cr−N$_{nitrido}$, the polarity of both σ and π density is insignificant, whereas the polarity of the σ and π density of Cr−O$_{oxo}$ and Cr−N$_{imido}$ is high. In other words, the -nitrido complex **3** has a stronger covalent π-bond character than the -oxo complex **4**. This result is also in accordance with the NBO analysis on M−O$_{oxo}$ and M−N$_{nitrido}$ bonds[33] with M = W, Mo, Re. Moreover, the Fermi hole distribution[34,35] both on σ (Figure 2a) and π (Figure 2b) direction in Cr−N$_{nitrido}$ bond also indicates the covalency between Cr and N$_{nitrido}$. The exact location of reference electron (given in the caption of Figure 2) is determined after trying out at various positions within the neighborhood of bonded maxinum.[36] Other three Cr−L multiple bonds all give similar feature in Fermi hole distribution.

TABLE 2: Natural Bond Orbital Analysis of Cr−L Multiple Bonds

	1, [(CO)$_4$(Cl)Cr≡CPh]			**4**, [(TPP)Cr≡O]		
bond	Cr−C$_{(carbyne)}$/1.725(4)[a]			Cr−O$_{(oxo)}$/1.582(4)[a]		
type	center	NHO	occ.	center	NHO	occ.
σ	Cr	sd$_{z^2}$ (35%)	1.921	Cr	sd$_{z^2}$ (20%)	1.832
	C$_{carbyne}$	sp$_z$ (65%)		O$_{oxo}$	sp$_z$ (80%)	
π_1	Cr	d$_{xz}$ (68%)	1.860	Cr	d$_{xz}$ (27%)	1.952
	C$_{carbyne}$	p$_x$ (32%)		O$_{oxo}$	p_x (73%)	
π_2	Cr	d$_{yz}$ (69%)	1.810	Cr	d$_{yz}$ (28%)	1.945
	C$_{carbyne}$	p$_y$ (31%)		O$_{oxo}$	p_y (72%)	
	2, [(bpb)Cr≡N]			**3**, [(bpb)(Cl)Cr≡N(CH$_3$)]		
bond	Cr−N$_{(nitrido)}$/1.555(2)[a]			Cr−N$_{(imido)}$/1.63(1)[a]		
type	center	NHO	occ.	center	NHO	occ.
σ	Cr	sd$_{z^2}$ (42%)	1.906	Cr	sd$_{z^2}$ (24%)	1.956
	N$_{nitrido}$	sp$_z$ (58%)		N$_{imido}$	sp$_z$ (76%)	
π_1	Cr	d$_{xz}$ (51%)	1.983	Cr	d$_{xz}$ (39%)	1.726
	N$_{nitrido}$	p$_x$ (49%)		N$_{imido}$	p$_x$ (61%)	
π_2	Cr	d$_{yz}$ (52%)	1.946	Cr	d$_{yz}$ (40%)	1.944
	N$_{nitrido}$	p$_y$ (48%)		N$_{imido}$	p$_y$ (60%)	

[a] Bond length of Cr−L multiple bond (Å).

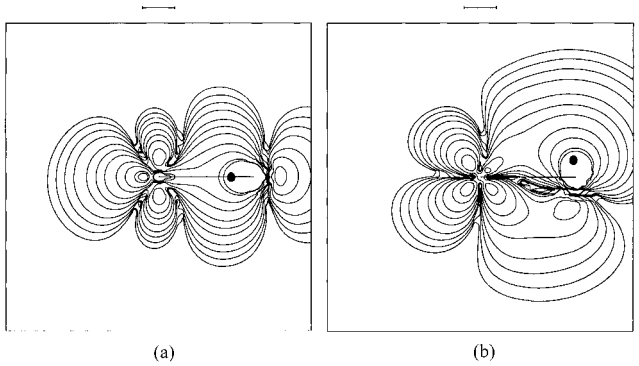

Figure 2. Fermi hole density with the reference electron (●) placed at 0.5 au away (a) and above (b) the N$_{nitrido}$ atom. The contours are in atomic unit with $-2^i \times 10^j$ (i = 0, 1, 2, 3; j = −3, −2, −1).

Laplacian of Electron Density. The Laplacian of the electron density, $\nabla^2\rho(\mathbf{r})$, identifies local charge concentrations (where $\nabla^2\rho(\mathbf{r}) < 0$) and local charge depletions ($\nabla^2\rho(\mathbf{r}) > 0$). It has been used to study the nature of chemical bond.[11,37] The Laplacian of density near the Cr nucleus is displayed in two projections shown in Figures 3 and 4 for **1** and **2**, respectively. The agreement between experiment and theory is adequate. The accumulation in the d_π directions and the depletion along the d_σ directions of Cr atom are clearly depicted in Figure 3a,b and Figure 4a,b. However, the discrepancies do exist in both **1** and **2**: A local charge concentration (CC) is observed along the

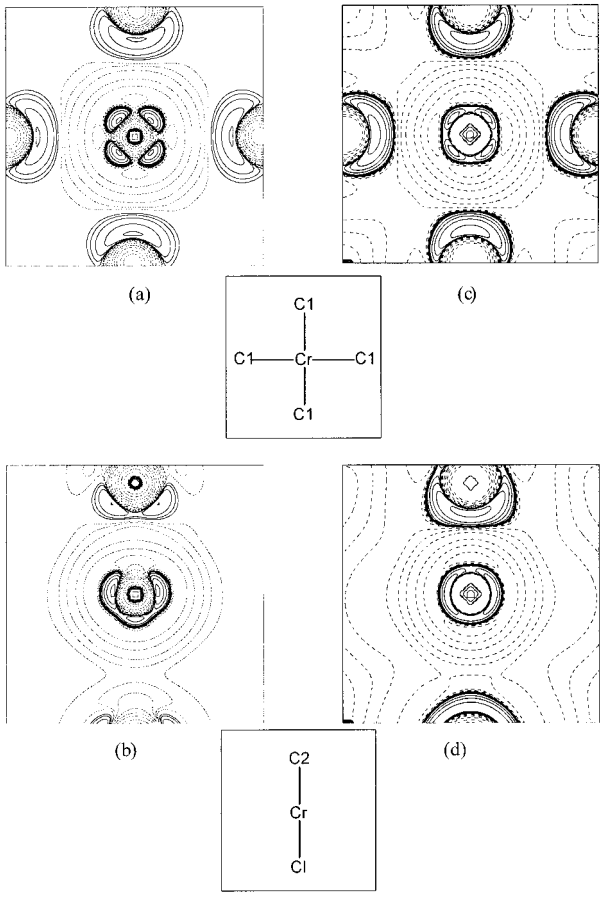

Figure 3. Laplacian maps of the *xy* plane (a,c) and *xz* plane (b,d) around the Cr center for compound **1**: (a), (b) from experiment; (c), (d) from DFT. (solid line, negative; dotted line, positive) The contour changes in steps of $(-1)^l 2^m 10^n$ ($l = 1, 0$; $m = 1-3$; $n = -2$ to $+2$).

Cr−Cl direction in experiment (Figure 3b) but not in theory (Figure 3d) of compound **1**. The feature around Cr at the projection of $Cr-N_{nitrido}$ in **2** is different in experiment (Figure 4b) and theory (Figure 4d). The effect of the size of the basis set on the metal i-VSCC was discussed[38] on the metal carbonyls (Cr, Fe, and Ni). But the discrepancies observed here are unlikely to be fully rationalized by the weakly pronounced feature mentioned therein. The Laplacian, $\nabla^2\rho$ around the Cr center and $Cr-N_{imido}$, $Cr-O_{oxo}$ bond of **3** and **4** from DFT calculation are shown in Figures 5 and 6, respectively. The feature at the horizontal plane (*xy*) are roughly the same for all four complexes; however, along the Cr−L bond, the local CC is only found around Cr toward the O_{oxo} ligand. The Laplacian at $C_{carbyne}$, $N_{nitrido}$, and N_{imido} atoms shows local CC toward the Cr. It is worth noticing that the i-VSCC of the Cr atom is in its third quantum shell,[19,20] and is topologically affected by the population of the 3d orbitals. The pattern of such CCs of the Cr atom could be the reflection of the uneven population among d-orbitals.[37,38] To show the shape of such i-VSCC around Cr, the isovalue surface of zero Laplacian ($\nabla^2\rho(\mathbf{r}) = 0$) around Cr atom is displayed in Figures 7−10, respectively, for complex **1**, **2**, **3,** and **4**. These surfaces simply give the relative description of the interfaces between the local charge concentrations and local charge depletions. In complex **1**, the surface around the chromium atom can be described as a pressed disk with four bumps located at the bisection of four carbonyl ligands both from experiment (Figure 7a) and theory (Figure 7b), there are six concaves toward each ligand. In complex **2**, a square pyramidal shape is observed where four bumps are located at

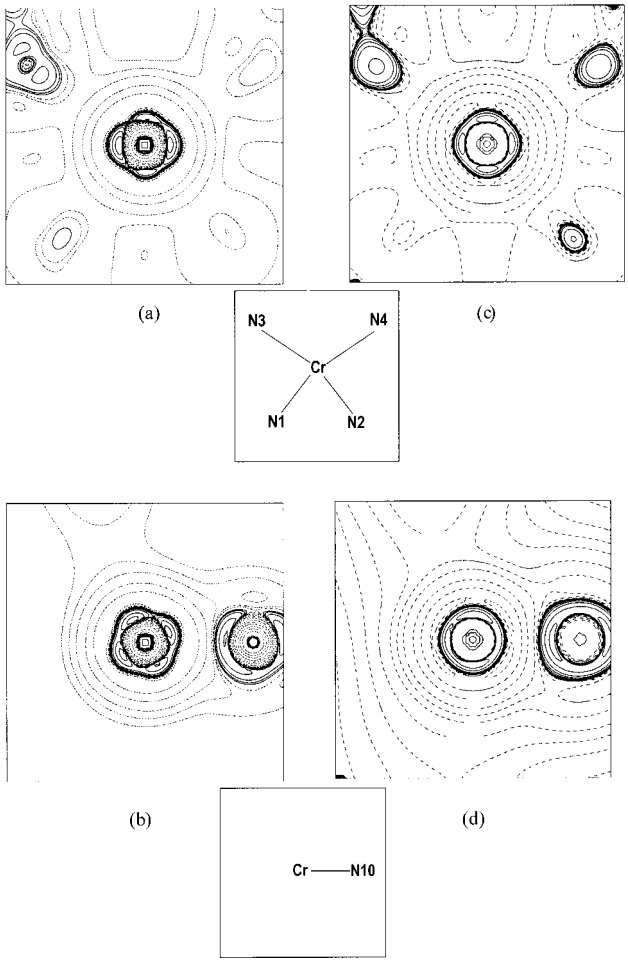

Figure 4. Laplacian maps of the *xy* plane (a,c) and *xz* plane (b,d) around the Cr center for compound **2**: (a), (b) from experiment; (c), (d) from DFT. The contours and plot sizes are as in Figure 3.

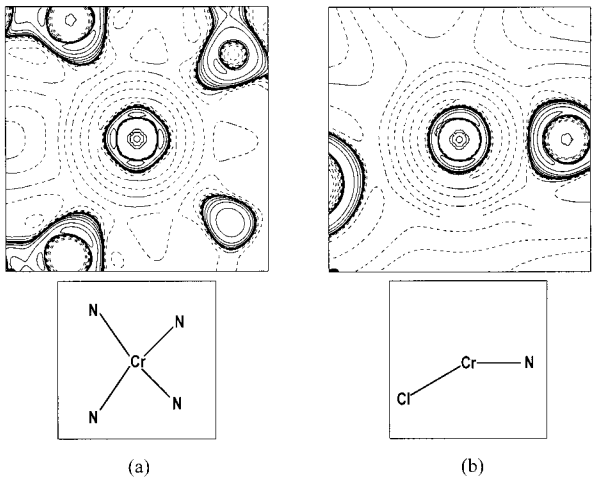

Figure 5. Laplacian maps of the *xy* plane (a) and *xz* plane (b) around the Cr center for compound **3** from DFT. The contours and plot sizes are as in Figure 3.

the bisection of $Cr-N_{bpb}$ bonds and one bump is found along $Cr-N_{nitrido}$ direction but opposite to the $N_{nitrido}$ shown in Figure 8. The similar charge distribution around Cr core can also be observed in $CrOF_4$ molecules.[39,40] The shape of the isovalue surface of zero Laplacian from experiment and from theory is basically the same, but the experimental surface shows clear separation between charge concentration and charge depletion.

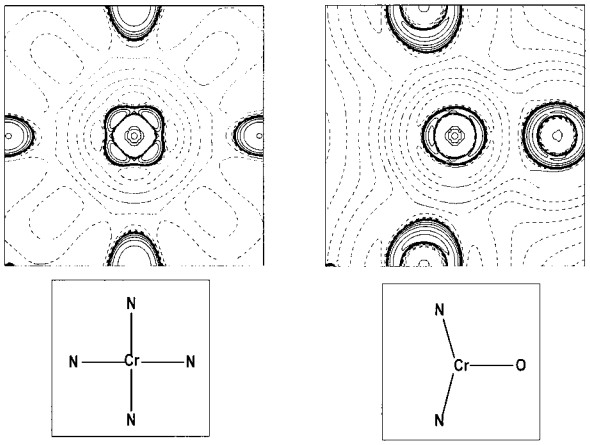

Figure 6. Laplacian maps of the *xy* plane (a) and *xz* plane (b) around the Cr center for compound **4** from DFT. The contours and plot sizes are as in Figure 3.

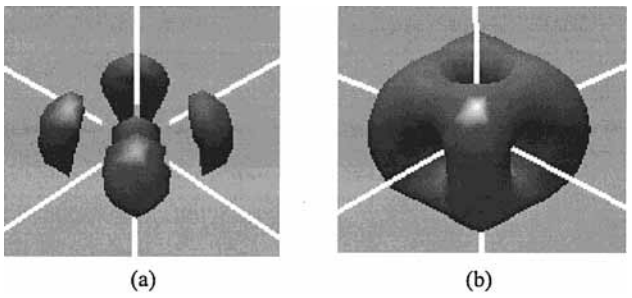

Figure 7. Isovalue surface of zero Laplacian ($\nabla^2\rho(r) = 0$) map at Cr of complex **1**, (a) from experiment, (b) from theory.

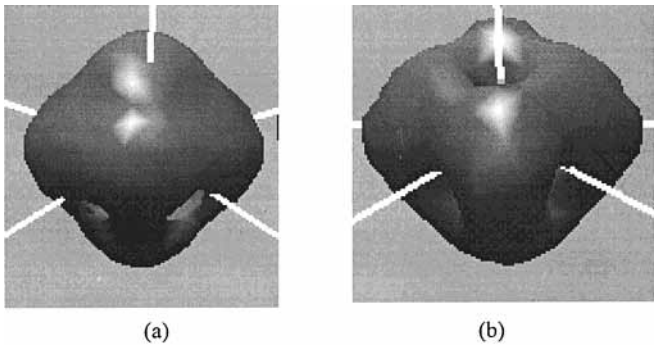

Figure 8. Isovalue surface of zero Laplacian ($\nabla^2\rho(r) = 0$) map at Cr of complex **2**, (a) from experiment, (b) from theory.

The surface in complex **3** shown in Figure 9 is similar to that of complex **1**. The surface in complex **4** shown in Figure 10 is somewhat peculiar. From the geometry of the coordination, it ought to be similar to that of **2**. However, there is an extra bump toward the O_{oxo}. This makes $Cr-O_{oxo}$ bond insert into a bump on this surface, whether this has anything to do with the high polarity of the bond is unclear at the moment. The same feature along $V-O_{oxo}$ bond was also observed[38] in $VOCl_3$.

The structure of the Laplacian of charge density for atoms in molecules[11,41] is most easily visualized in terms of the minimum in $\nabla^2\rho(\mathbf{r})$, a polyhedron whose numbers of vertexes (V), edges (E), faces (F) and the only cage critical point within the sphere obey the Poincaré−Hopf relationship.[41b] As a peculiar case, this is easily transformed into Euler's polyhedral formula[41c] $V - E + F = 2$. The local minimum (charge concentration, CC) in the valence shell of an atom defines the vertexes, V. The unique

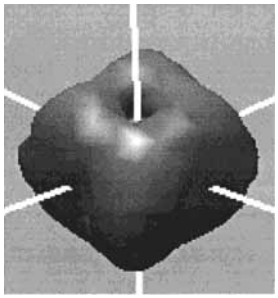

Figure 9. Isovalue surface of zero Laplacian ($\nabla^2\rho(r) = 0$) map at Cr of complex **3** from theory.

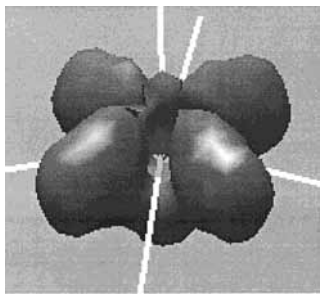

Figure 10. Isovalue surface of zero Laplacian ($\nabla^2\rho(r) = 0$) map at Cr of complex **4** from theory.

pair of trajectories of the gradient of $\nabla^2\rho(\mathbf{r})$ that originate at a (3, −1) critical point or saddle point between two minima and terminate at neighboring vertexes define the edges E of the polyhedron. The set of trajectories that arise at a (3, +1) critical point define the faces F of the polyhedron. The face critical points are where $\nabla^2\rho(\mathbf{r})$ attains a local maximum (charge depletion). This is called an atomic graph.[41] Generally, the ligands avoid the vertexes formed by CCs in the valence shell of a metal but are inserted in the faces of the polyhedron. Take **1** as an example, shown in Figure 7, there are four vertexes, eight edges, and six faces in chromium's i-VSCC, therefore satisfies the Eular's rule of $4 - 8 + 6 = 2$. It is understandable that each CC of six ligand atoms inserts toward one of the six faces. In the case of **2**, there are five vertexes, eight edges, and five faces. In the case of **3**, it is the same as in **1**. In the case of **4**, there are six vertexes, eight edges, and four faces. All the CCs of ligands are inserted toward the face, therefore the number of faces is the coordination number of the metal ion. As mentioned above, one exception is $Cr-O_{oxo}$ in **4** where the ligand O_{oxo} is toward a vertex instead of a face. We have not yet a good explanation for this, except the density polarization in this bond is highly polarized toward O_{oxo}.

Topological Properties of Bond Critical Points. Topological properties associated with BCPs of some typical covalent bonds of **1** and **2** are given in Table 3 from both experiment and theory. Those of Cr−L bonds are given in Table 1. The experimental $\rho(\mathbf{r_c})$ and $\nabla^2\rho(\mathbf{r_c})$ values are in good agreement with the theoretical ones, where $\mathbf{r_c}$ is the BCP. All C−C, C−O, and C−N bonds are definitely of covalent bond character (shared interaction),[42] having negative value of $\nabla^2\rho(\mathbf{r_c})$ and a greater than 1.0 of $\rho(\mathbf{r_c})$ value at the BCP, $\mathbf{r_c}$. The positive value of $\nabla^2\rho(\mathbf{r_c})$ of the C≡O bond found from the MO calculation in **1** can be rationalized by the highly polarized electron density on an extremely short bond,[11,43] since the BCP is only 0.37 Å away from C nucleus. In view of the complications to various bonding analyses based on the total electron density, it is also advantageous to use the local properties of the energy to analyze the bonding character.[44] For this purpose, the total energy density $H(\mathbf{r})$ is defined as $H(\mathbf{r}) = G(\mathbf{r}) + V(\mathbf{r})$, where $G(\mathbf{r})$ is a local

TABLE 3: Topological Properties Associated with BCP for Selected Intra-ligand Bonds of 1 and 2 (first line from experiment, second line from theory)

bonds	*d*1 Å	ρ(r) e Å^{-3}	$\nabla 2\rho$(r) e Å^{-5}	H_b (Hartree/Å^3)
		1		
C1−O1	0.394	3.774	−7.198	
	0.372	3.244	27.289	−5.962
C2−C3	0.715	1.668	−7.853	
	0.743	2.116	−24.368	−2.271
		2		
N3−C8	0.757	2.206	−15.646	
	0.886	2.210	−20.104	−3.579
C8−C9	0.709	2.212	−19.234	
	0.707	2.210	−21.903	−2.216
O1−C7	0.805	2.703	−13.751	
	0.827	2.643	−20.612	−4.491
N2−C6	0.740	2.100	−12.843	
	0.885	1.976	−21.466	−2.772
C1−C2	0.704	2.293	−23.018	
	0.718	2.122	−20.888	−2.147

kinetic energy, which is always positive, and $V(\mathbf{r})$ is the average field experienced by one electron in a many- particle system (or the local potential energy density), which is always negative. The sign of $H(\mathbf{r})$ determines whether the accumulation of charge at a point $\mathbf{r}$ is stabilizing [$H(\mathbf{r}) < 0$] or destabilizing [$H(\mathbf{r}) > 0$]. Investigation of a variety of chemical bonds revealed[44] that the covalent bonding feature (shared interaction) also can be characterized by a predominance of the local potential energy density $V(\mathbf{r})$ at the BCP reflected by $H(\mathbf{r_c}) \equiv H_b < 0$. On the other hand, the closed shell interactions, van der Waals interaction, or ionic bonds are characterized by a positive H_b.[11,44] Therefore, it is reasonable to say that the sign of H_b can provide bonding characterization in addition to the properties of $\rho(\mathbf{r_c})$, $\nabla^2\rho(\mathbf{r_c})$. For example, in the case of C≡O bond, although it has a positive $\nabla^2\rho(\mathbf{r_c})$, but it has a large $\rho(\mathbf{r_c})$ value (3.242 for theory) and a large negative H_b value (−5.96 Hartree/Å^3) (Table 3). This indicates the sign of the H_b can be taken as a sufficient condition for such a C≡O covalent bond. The values of topological properties of intra-ligand C−C, C−O, and C−N bonds in compound **3** and **4** are similar to those in compounds **1** and **2**. The topological properties associated with BCPs of $Cr-C_{carbyne}$, $Cr-N_{nitrido}$, $Cr-N_{imido}$, and $Cr-O_{oxo}$ multiple bonds together with some related bonds are summarized in Table 4. According to the concept of energy density H_b, it may be used as a qualitative measure for covalency of related M−L multiple bonds.[32,33] The larger the minus H_b value is, the stronger the covalent bond is.[33,42] The electron density at BCP, $\rho(\mathbf{r_c})$, as well as the value of H_b may provide a valid scale for the bond order or binding interaction of covalent bonds. For high-valent chromium complex **2**, **3,** and **4**, the $Cr-N_{nitrido}$ is characterized by a large $\rho(\mathbf{r_c})$ (2.057) value and a negative H_b value (−1.728 H Å^{-3}) of total energy density at the bond critical point, which indicates a strong covalent bond. The $Cr-O_{oxo}$ and $Cr-N_{imido}$ bonds are also covalent with negative values of H_b, −1.239 ($Cr-O_{oxo}$) and −0.823 ($Cr-N_{imido}$), but with less $\rho(\mathbf{r_c})$ values (1.827, 1.477) than that of $Cr-N_{nitrido}$ bond. This result is consistent with the NBO analysis and ESR studies of $Cr-O_{oxo}$ and $Cr-N_{nitrido}$ moiety. The nitrido complex has a stronger covalent π bond than the oxo complex based on ESR g values,[45] where the d_π orbitals (d_{xz}, d_{yz}) are destabilized in going from an oxo complex to a nitrido complex. The low-valent $Cr-C_{carbyne}$ bond of **1** is in covalent bond character with a negative H_b (−0.618 H Å^{-3}) and 1.228 e Å^{-3} in $\rho(\mathbf{r_c})$, which is stronger than the $Cr-C_{carbene}$ bond of the Fischer carbene complexes [$(CO)_5CrC(OMe)(C{\equiv}Cph)$][46] with −0.162 of H_b and 0.67 of $\rho(\mathbf{r_c})$. The same conclusion was drawn on the comparison of the $W-C_{carbyne}$[32a] and $W-C_{carbene}$[32b] bonds with the respective bond dissociation energy (BDE) of 155 and 75 kcal/mol. Topological properties of other Cr−L bond, such as Cr−Cl, $Cr-C_{carbonyl}$, $Cr-N_{amido}$, $Cr-N_{pyridyl}$, and $Cr-N_{pyrrole}$, are listed in Table 1. A small value in $\rho(\mathbf{r_c})$ and a positive value or a very small negative value in H_b are indicative of a closed shell interaction or ionic bond for these Cr−L bonds. Combining the NBO analysis, $\rho(\mathbf{r_c})$ and H_b values, the relative binding interaction of Cr−N bonds are in the order of $Cr-N_{nitrido} > Cr-N_{imido} > Cr-N_{amido} > Cr-N_{pyridine} \cong Cr-N_{pyrrole}$. It is also worth noticing that among the M−L multiple bonds of group VIB metals (M = Cr, Mo, W; L = N or O), the binding interaction is in the order of Mo−L > W−L > Cr−L on the basis of $\rho(\mathbf{r_c})$ and H_b values (Table 4).

Conclusion

Bonding characterization of Cr−L multiple bonds in four compounds are successfully accomplished by the NBO analysis and by the topological analysis on the total electron density. All four Cr−L multiple bonds display essentially a triple bond character consisting of one σ and two π bonds. On the basis of $\rho(\mathbf{r_c})$ and H_b values, the bond order or binding interaction of these multiple bonds is such that $Cr-N_{nitrido} > Cr-O_{oxo} > Cr-N_{imido} > Cr-C_{carbyne}$. It is demonstrated that $\rho(\mathbf{r_c})$ and H_b values can provide a good measure for binding interaction. The isovalue surface of zero Laplacian does give a good description of the shape of i-VSCC around the 3d transition metal ion.

TABLE 4: Topological Properties Analysis at the BCP of the M−L Multiple Bonds (first line from experiment, second line from theory)

bond	B.L. (Å)	d_1 (Å)	$\rho(r_c)$ (e Å^{-3})	$\nabla^2\rho(r_c)$ (e Å^{-5})	H_b	B.O.[a]	BDE (kcal/mol)	ref
$Cr-C_{carbyne}$	1.725	0.895	0.86	15.82				[c]
		0.896	1.23	13.88	−0.618	2.44	115.2[b]	
$W-C_{carbyne}$	1.843	1.015	1.22	10.44	−0.699		155.0	29
$Cr-C_{carbene}$	1.999	0.998	0.68	9.41				45
		0.973	0.67	9.02	−0.162		48.5	
$W-C_{carbene}$	2.088	1.065	0.77	7.46	−0.272		75.0	29
$Cr-N_{nitrido}$	1.555	0.846	1.87	26.94				[c]
		0.842	2.06	13.54	−1.728	2.72		
$Mo-N_{nitrido}$	1.728	0.959	2.49	10.14	−2.557			30
$W-N_{nitrido}$	1.727	0.934	2.27	14.45	−2.286			30
$Cr-N_{imido}$	1.630	0.847	1.48	23.92	−0.82	2.44		[c]
$Cr-O_{oxo}$	1.582	0.815	1.83	23.54	−1.239	2.65		[c]
$Mo-O_{oxo}$	1.755	0.932	2.15	21.07	−1.936			30
$W-O_{oxo}$	1.732	0.914	2.02	25.48	−1.741			30

[a] B.O. (bond order) = 1/2(occupancy of bonding orbitals − occupancy of antibonding orbitals) based on NBO analysis. [b] Ref 7, $[(CO)_5Cr(CCH_3)]$. [c] This work.

Acknowledgment. The authors thank the National Science Council of the Republic of China for the financial support. The authors also thank Dr. Anne Spasojevic-de Bire of Laboratorie de Chimie et Physico-Chimie Moleculaires, ERS 0070 du CNRS, Ecole Centrale Paris, France, for her supply of multipole coefficients and atomic parameters of chromium carbyne complex **1** (ref 12).

Supporting Information Available: Complete lists of topological properties at BCP of compound **1**, **2**, **3,** and **4**. Fermi hole distribution of compounds **1**, **3,** and **4**. This material is available free of charge via the Internet at http://pubs.acs.org.

References and Notes

(1) Fabius, B,; Cohen-Addad, C.; Larsen, C.; Lehman, M. S.; Becker, P. *J. Am. Chem. Soc.* **1989**, *111*, 5728.

(2) Bire, A. S.; Dao, N. Q.; Strich, A.; Thieffry, C.; Benard, M. *Inorg. Chem.* **1990**, *29*, 4908.

(3) Wang, Y.; Yeh, S. K.; Wu, S. Y.; Pai, C. T.; Lee, C. R.; Lin, K. J. *Acta Crystallogr.* **1991**, *B47*, 298.

(4) Lin, K. J.; Wang, Y. *J. Phys. Chem.* **1993**, *97*, 3176.

(5) Fan, J. M.; Wang, Y.; Ueng, C. H. *J. Phys. Chem.* **1993**, *97*, 8193.

(6) Coppens, P.; Abramov, Y.; Carducci, M.; Korjov, B.; Novozhilova, I.; Alhambra, C.; Pressprich, M. R. *J. Am. Chem. Soc.* **1999**, *121*, 2585.

(7) Kunze, K. L.; Hall, M. B. *J. Am. Chem. Soc.* **1986**, *108*, 5122.

(8) Schwarz, W. H. E.; Ruedenberg, K.; Mensching, L. *J. Am. Chem. Soc.* **1987**, *109*, 7617.

(9) Kunze, K. L.; Hall. M. B. *J. Am. Chem. Soc.* **1989**, *111*, 5728.

(10) Dunitz, J. D.; Seiler, P. *J. Am. Chem. Soc.* **1983**, *105*, 7056.

(11) Bader, R. F. W. *Atoms in Molecules, A Quantum Theory*; Oxford University Press: New York, 1990.

(12) Bire, A. S.; Dao, N. Q.; Fischer, E. O.; Hansen, N. K. *Inorg. Chem.* **1993**, *32*, 5354.

(13) Wang, C. C.; Wang, Y.; Chou, L. K.; Che, C. M. *J. Phys. Chem.* **1995**, *99*, 13899.

(14) (a) Lin, H. M.; Sheu, H. S.; Wang, C. C.; Che, C. M.; Wang, Y. *J. Chin. Chem. Soc.* **1999**, *46*, 487. (b) Lin, H. M.; Wang, C. C.; Che, C. M.; Wang, Y. Unpublished data.

(15) (a) Reed, A. E.; Weinhold, F. *J. Chem. Phys.* **1985**, *83*, 1736. (b). Foster, J. P.; Weinhold, F. *J. Am. Chem. Soc.* **1980**, *102*, 7211. (c). Reed, A. E.; Curtiss, L. A.; Weinhold, F. *Chem. Rev.* (Washington, DC) **1988**, *88*, 899. (d). Reed, A. E.; Weistock, R. B.; Weinhold, F. *J. Chem. Phys.* **1985**, *83*, 735. (e). Lwödin, P. O. *Phys. Rev.* **1955**, *97*, 1474.

(16) McWeeny, R. *Rev. Mod. Phys.* **1960**, *32*, 335.

(17) Bader, R. F. W.; Stephens, M. E. *Chem. Phys. Lett.* **1974**, *26*, 445.

(18) Bader, R. F. W.; Stephens, M. E. *J. Am. Chem. Soc.* **1975**, *97*, 7391.

(19) MacDougall, P. J.; Hall, M. B.; Bader, R. F. W.; Cheeseman, J. R. *Can. J. Chem.* **1989**, *67*, 1842.

(20) Bader, R. F. W.; Gillespie, R. J.; Martin, F. *Chem. Phys. Lett.* **1998**, *290*, 488.

(21) (a). Becke, A. D. *J. Chem. Phys.* **1993**, *98*, 5648. (b). Lee, C.; Yang, W.; Parr, R. G. *Phys. Rev.* **1988**, *B37*, 785.

(22) Frisch, M. J.; Trucks, G. W.; Schlegel, H. B.; Scuseria, G. E.; Robb, M. A.; Cheeseman, J. R.; Zakrzewski, V. G.; Montgomery, J. A.; Stratmann, R. E.; Burant, J. C.; Dapprich, S.; Millam, J. M.; Daniels, A. D.; Kudin, K. N.; Strain, M. C.; Farkas, O.; Tomasi, J.; Barone, V.; Cossi, M.; Cammi, R.; Mennucci, B.; Pomelli, C.; Adamo, C.; Clifford, S.; Ochterski, J.; Petersson, G. A.; Ayala, P. Y.; Cui, Q.; Morokuma, K.; Malick, D. K.; Rabuck, A. D.; Raghavachari, K.; Foresman, J. B.; Cioslowski, J.; Ortiz, J. V.; Stefanov, B. B.; Liu, G.; Liashenko, A.; Piskorz, P.; Komaromi, I.; Gomperts, R.; Martin, R. L.; Fox, D. J.; Keith, T.; Al-Laham, M. A.; Peng, C. Y.; Nanayakkara, A.; Gonzalez, C.; Challacombe, M.; Gill, P. M. W.; Johnson, B. G.; Chen, W.; Wong, M. W.; Andres, J. L.; Head-Gordon, M.; Replogle, E. S.; Pople, J. A. *Gaussian 98* (Revision A.7); Gaussian, Inc.: Pittsburgh, PA, 1998.

(23) Wachters, A. J. H. *J. Chem. Phys.* **1970**, *52*, 1033.

(24) Rappe, A. K.; Smedley, T. A.; Goddard, W. A., III. *J. Phys. Chem.* **1981**, *85*, 2607.

(25) Zeigler, T. *Chem. Rev.* **1991**, *91*, 651.

(26) Andzelm, J. W.; Wimmer, E. *J. Chem. Phys.* **1992**, *96*, 1280.

(27) Salahub, D. R.; Zerner, M. C. In *The Challenge of d and f electrons: Theory and Computation*; Eds.; *ACA Symposium Series 394*; American Chemical Society; Washington, DC, 1989; p 165.

(28) Gatti, C.; MacDougall, P. J.; Bader, R. F. W. *J. Chem. Phys.* **1988**, *88*, 3792.

(29) Hansen, N. K.; Coppens, P. *Acta Crystallogr.* **1978**, *A34*, 909.

(30) PROP program: A program developed by M. Souhassou, N. K. Hansen, E. Stevens, B. Craven, N. Bouhmeida, N. Ghermani, and C. Lecomte.

(31) AIMPAC: a set of programs for the Theory of *Atom in Molecules*; Bader, R. F. W., and co-worker, Eds.; McMaster University: Hamilton, Ontario, Canada, 1994.

(32) (a) Vyboishchikov, S. F.; Frenking, G. *Chem. Eur. J.* **1998**, *4*, 1439. (b). Vyboishchikov, S. F.; Frenking, G. *Chem. Eur. J.* **1998**, *4*, 1428.

(33) Neuhaus, A.; Veldkamp, A.; Frenking, G. *Inorg. Chem.* **1994**, *33*, 5278.

(34) Bader, R. F. W.; Streitwieser, A.; Neuhaus, A.; Laidig, K. E.; Speers, P. *J. Am. Chem. Soc.* **1996**, *118*, 4959.

(35) Bader, R. F. W.; Johnson, S.; Tang, T.-H.; Popelier, P. L. A. *J. Phys. Chem.* **1996**, *100*, 15398.

(36) Bader, R. F. W.; Gillespie, R. J.; MacDougall, P. J. *J. Am. Chem. Soc.* **1988**, *110*, 7329.

(37) Lee, C. R.; Wang, C. C.; Chen, K. C.; Lee, G. H.; Wang, Y. *J. Phys. Chem. A* **1999**, *103*, 156.

(38) MacDougall, P. J.; Hall, M. B. *Trans. Am. Crystallogr. Assoc.* **1990**, *26*, 105.

(39) Gillespie, R. J.; Robinson, E. A. *Angew. Chem., Int. Ed. Engl.* **1996**, *35*, 495.

(40) Gillespie, R. J.; Bytheway, I.; Tang, T.-H.; Bader, R. F. W. *Inorg. Chem.* **1996**, *35*, 3954.

(41) (a) Bader, R. F. W.; MacDougall, P. J. *J. Am. Chem. Soc.* **1985**, *107*, 6788. (b) Collard, K.; Hall, G. G. *Int. J. Quantum Chem.* **1977**, *12*, 623. (c) Bader, R. F. W.; Popelier, P. L. A.; Chomg, C. *J. Mol. Struct. (THEOCHEM)* **1992**, *255*, 145.

(42) Bader, R. F. W.; Essén H. *J. Chem. Phys.* **1984**, *80*, 1943.

(43) Slee, T. *J. Am. Chem. Soc.* **1986**, *108*, 606.

(44) (a) Cremer, D.; Kraka, E. *Angew. Chem., Int. Ed. Engl.* **1984**, *23*, 627. (b) Cremer, D.; Kraka, E. *Croat. Chem. Acta* **1984**, *57*, 1259.

(45) Fujii, H.; Yoshimura, T.; Kamada, H. *Inorg. Chem.* **1997**, *36*, 1122.

(46) Wang, C. C.; Wang, Y.; Liu, H. J.; Lin, K. J.; Chou, L. K.; Chan, K. S. *J. Phys. Chem.* **1997**, *101*, 8887.